

THE APPLICATION OF JET IMPINGEMENT FOR PISTON COOLING

Nasif G.,* Barron R.M. and Balachandar R.

*Author for correspondence

Department of Mechanical, Automotive & Material Engineering

University of Windsor

Windsor, Ontario

Canada

E-mail: nasifg@uwindsor.ca

ABSTRACT

The impinging jet is regarded as a method of achieving high convective heat transfer coefficients and therefore enhancing the heat transfer from the inner shell of the piston, particularly from the impingement and its neighboring regions. In this study, a transient numerical investigation has been carried out to evaluate the piston cooling process due to oil jet impingement. The volume of fluid method utilizing a high resolution interface capturing scheme was used to perform the two-phase (air-oil) simulations. The governing 3D Navier-Stokes equations and energy equation are numerically solved using a finite volume discretization. The conjugate heat transfer method is used to obtain a coupled heat transfer solution between the solid and fluid, to predict the heat transfer coefficient. Two engine speeds are used in the simulations, i.e., when the engine is operating at a normal condition (2000 rpm) and when the engine is operating at a full load condition (6000 rpm). It is shown that the cooling jet can considerably decrease the volume and surface average temperature of the piston.

INTRODUCTION

In internal combustion engines, the combustion of fuel occurs with air in a combustion chamber. The expansion of the high temperature and high pressure gases produced by combustion apply direct force to some components of the engine, most notably on the pistons. This force moves the piston, transforming chemical energy into useful mechanical energy. The piston is the only part of the combustion chamber that is not cooled by the standard traditional methods. In the automotive industry, there is a continuous need for increasing engine performance concurrently with decreasing free space in the engine compartment. One of the consequences of increasing the engine power is that it threatens the structural integrity of the pistons. Internal combustion engine pistons can be cooled by oil, water or air jets. Air-cooling is simpler from a design point of view, but lower specific heat per unit volume of air requires very large quantities of air to be directed towards the piston. This involves huge ducting arrangements and an additional air compressor, which makes it less appealing from a practical viewpoint. Water-cooling was applied to heavy, low speed engines, but later it was abandoned because of serious

design and maintenance difficulties with piping and sealing. Oil jet piston cooling has recently been adopted as an alternative and efficient way to cool the piston.

NOMENCLATURE

BDC	Bottom dead center
d	Nozzle diameter
H	Nozzle-to-disc spacing
HTC (or) h	Heat transfer coefficient
k	Turbulent kinetic energy
N	Rotational speed, rpm
q_w''	Convective heat flux
Re_d	Reynolds number of the jet = $v_f d / \nu_{oil}$
r	Radial distance measured from the jet axis
RANS	Reynolds Averaged Navier-Stokes
T	Temperature
T_f	Jet temperature at nozzle exit
T_{ref}	Reference temperature
T_w	Wall temperature
TDC	Top dead center
u_r, v_z	Velocity components in cylindrical coordinates
v_f	Bulk velocity at the nozzle exit
Special characters	
μ	Dynamic viscosity
ν	Kinematic viscosity = μ_{oil} / ρ_{oil}
ρ	Density
ω	Specific dissipation rate

A significant amount of research has been reported in the open literature [1–3] on jet impingement heat transfer, which is widely used for a variety of heating and cooling applications. Martin [4] and Jambunathan et al. [5] conducted a thorough review of heat transfer research related to impinging jets for such applications. Most of the studies were performed using a single jet or array of jets impinging onto a stationary flat plate. A numerical study to investigate the thermal characteristics of impinging jet onto a fixed disc placed in a confined cylindrical space and subjected to uniform heat flux on the surface was carried out in [6], using different nozzle diameters and flow conditions. The research revealed that the normalized local Nusselt number had a distinct dependence on the radial location and only a slight dependence on the Reynolds number. An experimental study to characterize the heat transfer coefficient

(HTC) for round fully-developed turbulent liquid jets impinging normally onto a uniform heat flux surface was carried out by Stevens & Webb [7,8] with varying nozzle diameters and flow conditions. Their investigation revealed that the Nusselt number in the region near the stagnation point was primarily dependent on Reynolds number, Re_d , Prandtl number, Pr , and radial velocity gradient, $\partial u_r / \partial r$, and less dependent on nozzle-to-target spacing, H .

The current computational study involves jet impingement heat transfer onto a high-speed moving boundary. The transient simulation of such a problem is challenging and computationally costly. To overcome the high computational cost, Nasif et al. [9] established an innovative approach to accelerate the solution. The acceleration procedure involves several stages, including the simulation of the heat transfer of a stationary disc with a cooling jet at different impingement distances from the nozzle exit. Using data from these simulations, the flow field and thermal characteristics of a reciprocating moving disc with constant heat flux and an impinging cooling jet is then considered. The acceleration methodology is used in the current study to expedite the computational solution.

The objective of the present study is to numerically evaluate the performance of the cooling process when an oil jet (SAE 5W30) impinges perpendicularly onto a reciprocating moving piston. Pipe nozzle sizes in the range $d = 1.0 \text{ mm} - 3.0 \text{ mm}$, for a wide range of issuing velocities, are employed in the simulations. A piston motion equation is used to capture the reciprocating motion of the piston within a piston stroke of 82.0 mm. Two engine speeds (N) are used in the simulations, i.e., when the engine is operating at a normal condition ($N = 2000 \text{ rpm}$) and the engine is operating at a full load condition ($N = 6000 \text{ rpm}$).

NUMERICAL METHOD

Finite volume computations using CD-adapco's STAR-CCM+ [10] with polyhedral cells are performed in the current study. First-order implicit time marching and second-order spatial differencing schemes are used to discretize the governing partial differential equations. A segregated flow model, which solves the flow equations (one for each component of velocity, and one for pressure) in an uncoupled manner, is used to solve the discretized equations. The linkage between the momentum and continuity equations is achieved with a predictor-corrector approach. The complete formulation can be described as an implementation on a collocated variable arrangement with a Rhie and Chow pressure-velocity coupling combined with a SIMPLE algorithm [10].

The $k-\omega$ SST turbulence model is a two-equation eddy viscosity model that has been shown to be more accurate in capturing wall effects than other RANS models, and has therefore been selected as the turbulence model in this study. The $k-\omega$ SST model solves additional transport equations for turbulent kinetic energy k and specific dissipation rate ω , from which the turbulent viscosity ($\nu_t = k/\omega$) can be derived. The transport equations for k and ω are described in [10,11].

Since the flow field under investigation involves two immiscible fluids (oil jet in compressible air), a numerical model to handle two-phase flow is required. Volume of fluid (VOF) [12] is a simplified multiphase approach that is well suited to simulate flows of several immiscible fluids and is capable of resolving the interface between the mixture phases. In a VOF simulation, the basic model assumption is that all phases share the same velocity and pressure and no additional modelling of inter-phase interaction is required. The normalized variable diagram provides the methodology used in constructing high-resolution schemes [13]. The Compressive Interface Capturing Scheme for Arbitrary Meshes (CICSAM) [14] and the High-Resolution Interface Capturing Scheme (HRIC) [15] are the most commonly used high-resolution schemes for interface capturing with the VOF model. The HRIC scheme is used to capture the interface in the present work. In high-resolution schemes, an additional condition, the convective boundedness criterion, must be satisfied along with the local Courant-Friedrichs-Lewy (CFL) condition. The CFL condition is a necessary condition for numerical stability. If an explicit time marching solver is used, then a Courant number less than one is typically required. Implicit solvers, like the one used in this study, are less sensitive to numerical instability and larger values of Courant number may be tolerated [10].

The interaction between the heat conduction inside the solid and the flow of fluid adjacent to the fluid-solid interface is commonly referred to as a conjugate heat transfer process [16-18]. The conjugate heat transfer method allows for a coupled heat transfer solution between the solid and fluid, and predicts the heat transfer coefficient more accurately than a decoupled solution. The conjugate heat transfer technique is used in the current simulation to estimate the heat transfer coefficient on the solid surface due to the impingement of the oil jet.

The current simulations involve a moving boundary. Therefore, a morphing process is used to redistribute the mesh vertices in response to the movement of the control points. Control points and their associated displacements are used by the mesh morpher to generate an interpolation field throughout the region which can then be used to displace the actual vertices of the mesh. Each control point has an associated distance vector, which specifies the displacement of the point within a single time-step [10].

Problem Setup and Boundary Conditions

The present transient numerical simulation is used to predict the steady thermal characteristics when an oil jet impinges orthogonally onto a reciprocating piston. The physical domain with relevant boundary conditions is shown in Figure 1. Two engine speeds are employed in the current simulations, i.e., $N = 2000$ and 6000 rpm , with three pipe nozzles of sizes $d = 1.0, 2.0$ and 3.0 mm , corresponding to bulk issuing velocities in the range $10 \text{ m/s} \leq v_f \leq 60 \text{ m/s}$. Pipe flows were initially simulated to generate fully developed flow profiles, which were then taken as the inlet boundary condition to the computational domain. The oil exits the nozzle with a temperature of $90 \text{ }^\circ\text{C}$, flows as a jet towards the piston and spreads out along the piston inner surface, as shown in Figure 1 (Section A-A). The

mesh is clustered at the jet trajectory to prevent the smearing of the oil. For better capturing of the air-oil interfaces and to accurately compute the HTC, prism layers at near wall locations are packed in 0.4 mm width with a stretching factor of 1.25, producing a y^+ value less than 3.5, as shown in Figure 1 (Detail A). The validation process and criteria for choosing the cell count are based on our previous studies [6, 9] and are not repeated here for brevity.

The top surface of the piston is subjected to convective heat transfer due to the hot gases in the combustion chamber. The temperature distribution with corresponding average heat transfer coefficients over the cycle are given in Figure 1. The cylinder wall is kept at constant temperature over the engine cycle, i.e., $T = 130^\circ\text{C}$ and 180°C , corresponding to engine speeds $N = 2000$ and 6000 rpm, respectively. All oil and air properties, i.e., dynamic viscosity, density, thermal conductivity and specific heat are evaluated as functions of the local temperature in the computational domain. A portion of combustion gases also infiltrates as blow-by gases through the clearance between the piston and cylinder to the crankcase. The mass flow rate and temperature of the blow-by gases are given in Figure 1 (Section A-A). The transient boundary conditions as a function of the crank angle at the bottom of the cylinder, i.e., pressure, temperature, velocity components and turbulent intensities are extracted from a full scale engine simulation without a cooling jet [19].

The time step for the simulations was set to a crank angle of 0.5° for both engine speeds, with five internal iterations at each time step. The CFL condition, which is required for numerical stability with the volume of fluid model, is achieved with this time step, i.e., the maximum local Courant number is less than 1.0 everywhere in the computational domain. The thermal contact of conductance between the piston and the compression rings (Detail B in Figure 1) is taken as $50000.0 \text{ W/m}^2\cdot\text{K}$ [20].

The convective HTC is conveniently expressed as [20]:

$$h = q''_w / (T_w - T_{ref}) \quad (1)$$

The convective heat transfer coefficient in Equation (1) is evaluated based on a specific bulk or reference temperature (T_{ref}). In the current study the jet issuing temperature of 90°C was chosen as a reference temperature. More details on the evaluation of the convective heat transfer coefficient at the fluid-solid interface using the wall thermal law can be found in [10].

The piston motion equation, which produces a reciprocating motion of the piston, is given as:

$$v_{piston} = r_c \sin \theta_c - \frac{r_c^2 \sin \theta_c \cos \theta_c}{\sqrt{l^2 - r_c^2 \sin^2 \theta_c}} \quad (2)$$

where v_{piston} is the linear velocity of the piston, l is the rod length, r_c is the crank radius, and θ_c is the crank angle (from the cylinder bore centerline and TDC).

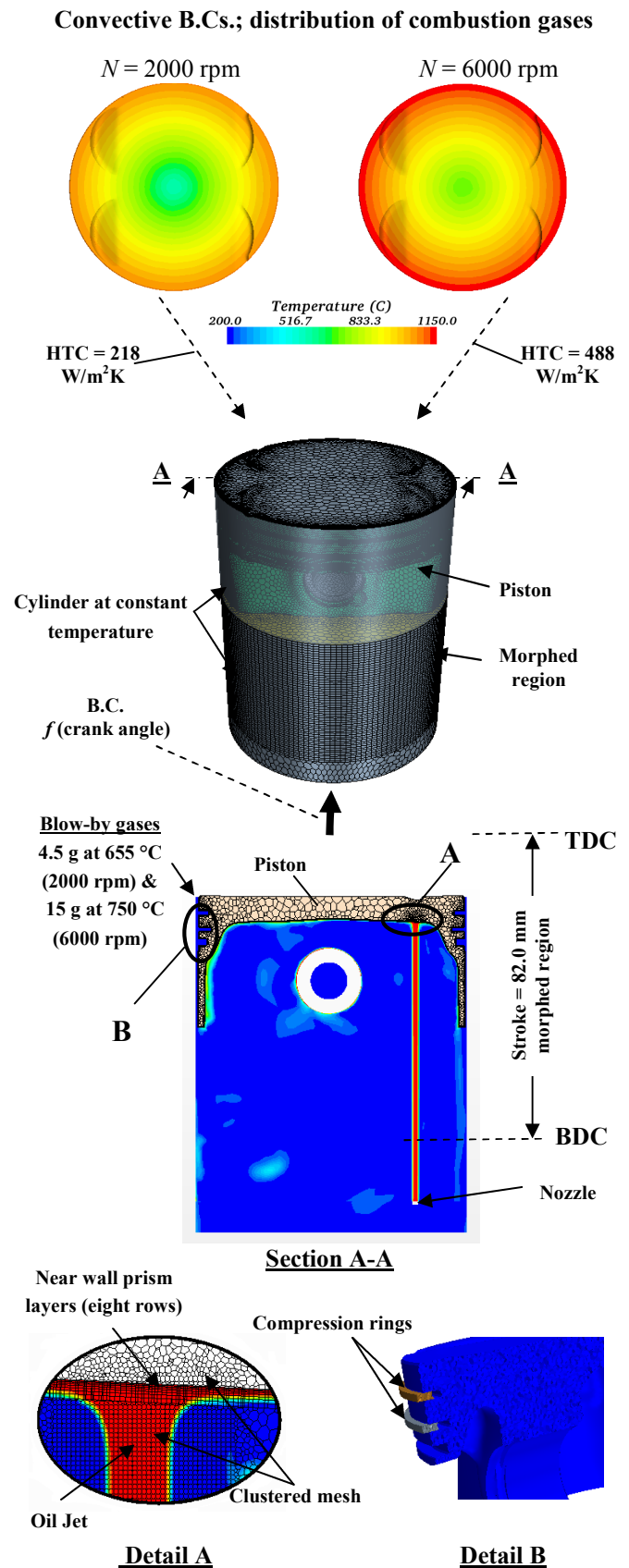


Figure 1 Computational domain with relevant boundary conditions

RESULTS

A proper understanding of the HTC distribution over the piston surface can be gained by splitting the exterior and interior surfaces of the piston into patches as shown in Figure 2. Each colour in this figure represents a separate region. Figure 3 shows the transient surface average HTC profiles as function of the crank angle or time (only the last 5 cycles from the simulation are shown) for the regions defined in Figure 2. The physical time for one cycle (360°) is 0.03 and 0.01 s corresponding to the two engine speeds, i.e., $N = 2000$ and 6000 rpm, respectively. Only a few selected cases using one nozzle exit velocity, $v_f = 45$ m/s, are shown in this figure.

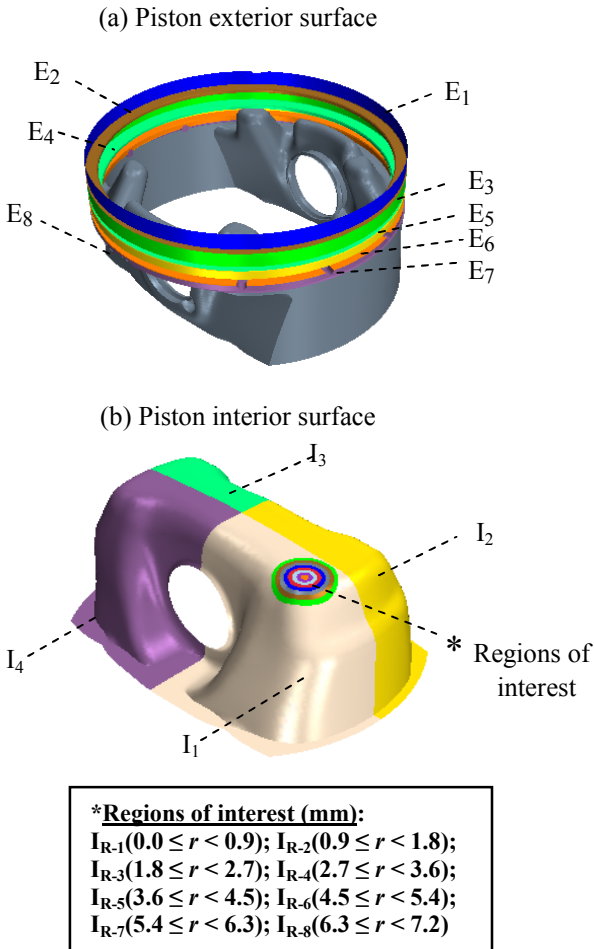


Figure 2 Piston configuration; (a) exterior shell; (b) interior shell

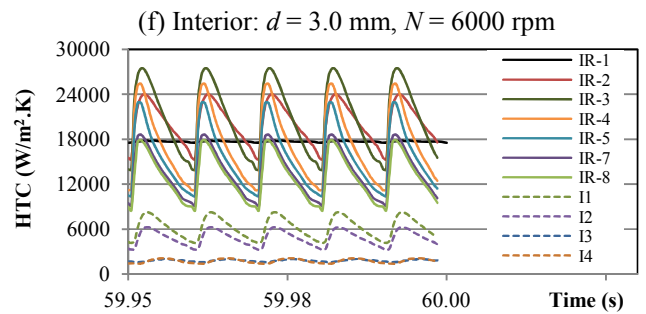
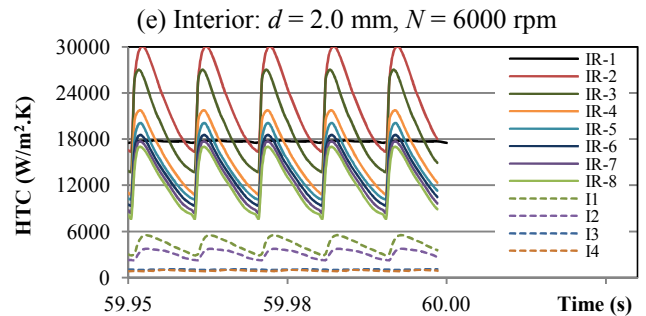
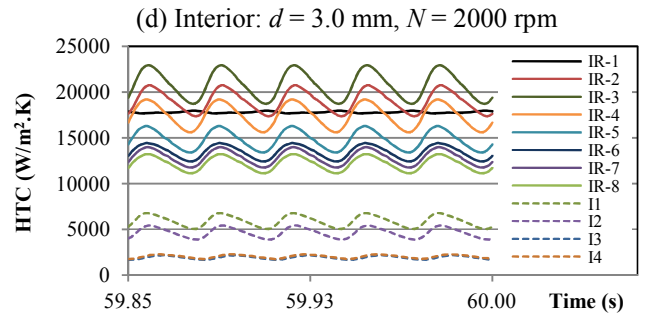
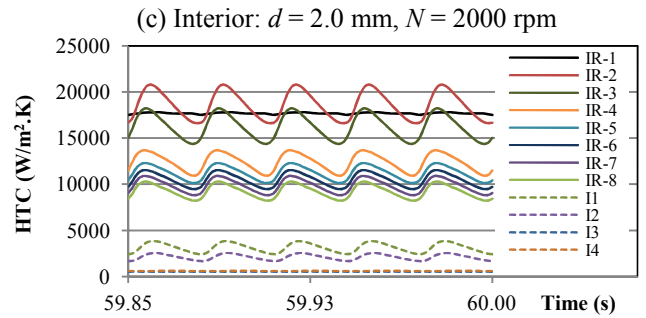
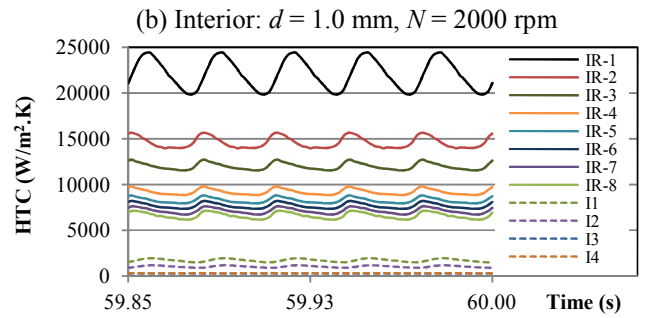
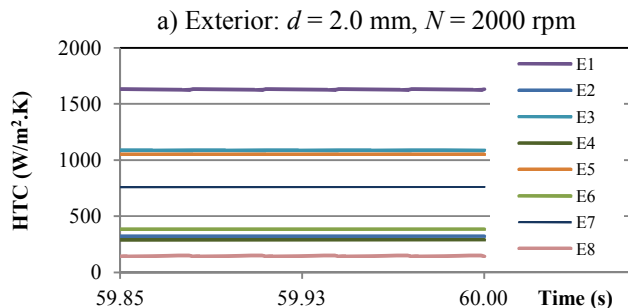


Figure 3 HTC profiles for the regions given in Figure 2, the nozzle exit velocity is 45 m/s

The heat transfer into the piston exterior shell occurs due to the high temperature of the combustion and blow-by gases, while the heat transfer from the interior shell of the piston occurs mainly due to the relatively low temperature of the oil, which spreads over the surface after jet impingement. The HTC profile at the exterior shell is constant over the cycle as shown in Figure 3a. Unlike the exterior shell, the HTC profile at the interior shell is recurring and a function of the crank angle as shown in Figure 3b-f. This repetitive feature can be attributed to the relative velocity between the impinging jet and piston. Some relevant observations can be drawn from Figure 3; first, the value of HTC is higher at the piston interior surface compared with the exterior surface, due to the higher Pr and specific heat per unit volume of the oil which enhances the HTC at the interior surface of the piston. Second, the HTC profile at the interior surface tends to be constant over the cycle in a small region around the impingement point, i.e., region I_{R-1} marked in Figure 2, when the size of the nozzle exceeds the size of this region as shown in Figure 3c-f (black curve). Third, the occurrence of maximum HTC is shifted away from the impingement point as the nozzle size increases; this observation is clearly shown in Figure 3c-f. The maximum HTC (red curve) in Figure 3c and 3e occurs in the region I_{R-2} , whereas the nozzle size is $d = 2.0$ mm. The maximum HTC (dark green curve) in Figure 3d and 3f occurs in the region I_{R-3} , whereas the nozzle size is $d = 3.0$ mm. The heat transfer coefficient is strongly dependent on the radial velocity gradient adjacent to the wall [8-9], i.e., $(\partial u_r / \partial r)_{r \rightarrow 0}$, where u_r is the radial velocity of the fluid and r is the radial extent from the impingement point. The occurrence of the maximum radial velocity gradient moves away from the impingement point as the nozzle size increases [6,9], this is reflected in the shifting of the maximum HTC with the nozzle size. The HTC profile at the interior surface of the piston shows a difference between the maximum and minimum values of HTC during the cycle, and that this difference increases with the engine speed due to the increase of the relative velocity between the jet and piston.

The investigations that were carried out in [8] suggest that the parameter v_f/d may be used to functionally specify the HTC in a region immediately around the impingement point. Figure 4 shows the effect of the parameter v_f/d on the HTC at the region I_{R-1} . Irrespective of the nozzle size, the HTC in this region increases with the parameter v_f/d .

One of the consequences of the jet impingement is the increase of the convective heat transfer at the top surface of the piston. The amount of heat passing into the piston increases with the jet Reynolds number as illustrated in Figure 5, which clearly shows that the convective heat transfer is entirely a function of the jet Reynolds number when the engine is operating at normal condition, i.e., 2000 rpm, while it is a function of both jet Reynolds number and nozzle size when the engine is operating at full load condition, i.e., 6000 rpm. The temperature difference between the surroundings and the solid piston is higher with the cooling jet. This will increase the convective heat transfer into the outer surface of the piston from the combustions gases.

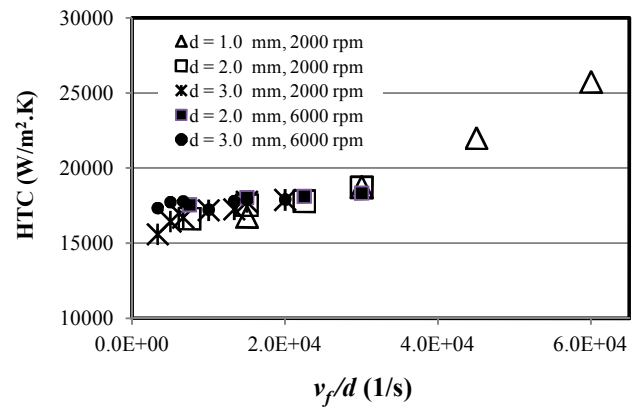


Figure 4 Effect of v_f/d on the HTC in the region around the impingement point (i.e., $0.0 \leq r < 0.9$)

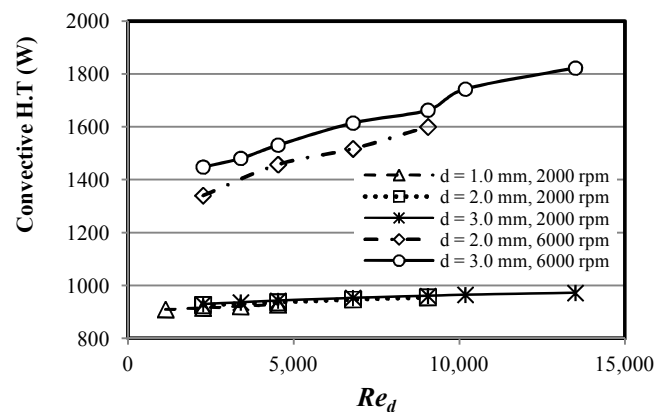


Figure 5 Convective heat transfer at the top surface of the piston

The piston volume average temperature for an engine running at normal condition without cooling jet is 225°C . The contour of highest temperature (not shown here) appears in the region beneath the exhaust valve ("Region of interest" in Figure 2). With the cooling jet, the contour of highest temperature is shifted towards the left edge of the piston, in the region below the intake valves. However, this temperature remains less than the temperature at the same corresponding location in the case of no jet. Figure 6 shows the effect of jet Reynolds number on the piston volume and interior surface average temperatures for both engine speeds. For given Reynolds number and when the engine is operating at normal condition, the average temperature in the piston is independent of nozzle size and slightly dependent on Reynolds number when $Re_d > 7500$. However, the actual temperature distribution does change with nozzle size (contours are not shown here). Contrary to the engine operating at a normal condition, the piston volume and surface average temperatures are functions of both Reynolds number and nozzle size when the engine is operating at full load condition, as shown in Figure 6a and 6b.

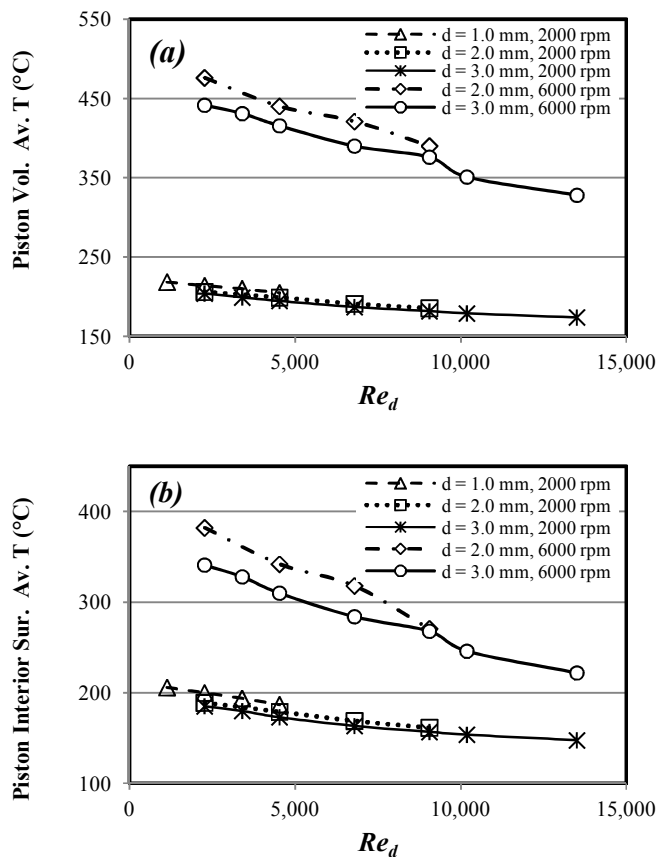


Figure 6 Effect of jet Re_d on: (a) piston volume average temperature, (b) piston interior surface average temperature

CONCLUSIONS

In this study, an automotive engine application of the cooling oil jet is evaluated using finite volume analysis. Simulation of an oil jet impinging onto a high-speed moving piston was carried out using the volume of fluid method. Two engine operating speeds, i.e., 2000 and 6000 rpm were employed in the simulations. The conclusions can be summarized as follow:

- The HTC profile at the piston interior surface tends to be constant over the cycle in a small region around the impingement point when the size of the nozzle exceeds the size of this region.
- The occurrence of maximum HTC is shifted away from the impingement point as the nozzle size increases.
- The jet impingement cooling process will increase the convective heat transfer from the combustion gases to the piston top surface.
- Both piston volume and piston interior surface average temperatures are only function of Reynolds number when the engine is operating at normal condition. However, the average temperature is a function of both Reynolds number and nozzle size when the engine is operating at full load condition.

REFERENCES

- [1] Cornaro, C., Fleischer, A.S., Rounds, M., and Goldstein, R.J., Jet impingement cooling of a convex semi-cylindrical surface, *Int. J. Therm. Sci.*, Vol. 40, pp. 890–898, 2001.
- [2] Gau, C., and Chung, C.M., Surface curvature effect on slot-air-jet impingement cooling flow and heat transfer process, *J. Heat Transfer*, Vol. 113 (4), pp. 858–864, 1991.
- [3] Wolf, D.H., Incropera, F.P., and Viskanta, R., Jet impingement boiling, *Advances in Heat Transfer*, Vol. 23, pp. 1-132, 1993.
- [4] Martin, H., Heat and mass transfer between impinging gas jets and solid surfaces, *Advances in Heat Transfer*, Vol. 13, pp. 1-60, 1977.
- [5] Jambunathan, K., Lai, E., Moss, M.A., and Button, B.L., A review of heat transfer data for single circular jet impingement, *Int. J. Heat Fluid Flow*, Vol. 13 (2), pp. 106–115, 1992.
- [6] Nasif, G., Barron, R.M., and Balachandar, R., Heat transfer due to an impinging jet in a confined space, *J. Heat Transfer*, 136(11), doi:10.1115/1.4028242, 2014.
- [7] Steven, J., and Webb, B.W., The effect of inclination on local heat transfer under an axisymmetric, free liquid jet, *Int. J. Heat Mass Transfer*, Vol. 34(4-5), pp. 1227–1236, 1991.
- [8] Steven, J., and Webb, B.W., Local heat transfer coefficient under an axisymmetric, single-phase liquid jet, *J. Heat Transfer*, Vol. 113(1), pp. 71–78, 1991.
- [9] Nasif, G., Barron, R.M., and Balachandar, R., Simulation of jet impingement heat transfer onto a moving disc, *Int. J. Heat and Mass Transfer*, Vol. 80, pp. 539-550, 2015.
- [10] CD-adapco, STAR-CCM+ V7.02.008, User Manual, 2012.
- [11] Hoffmann, K., and Chiang, S., *Computational Fluid Dynamics-Vol. 3*, 4th Edition, Engineering Education System, Wichita, KS, USA, 2000.
- [12] Hirt, C.W., and Nichols, B.D., Volume of fluid (VOF) method for the dynamics of free surfaces, *J. Computational Physics*, Vol. 39, pp. 201-225, 1981.
- [13] Leonard, B.P., The ULTIMATE conservative difference scheme applied to unsteady one-dimensional advection, *Computer Methods in Applied Mechanics and Engineering*, Vol. 88, pp. 17-74, 1991.
- [14] Ubbink, O., and Issa, R.I., Method for capturing sharp fluid interfaces on arbitrary meshes, *J. Computational Physics*, Vol. 153, pp. 26-50, 1999.
- [15] Muzafferija, S., Peric, M., Sames, P., and Schelin, T., A two-fluid Navier-Stokes solver to simulate water entry, *Proceedings of Twenty-Second Symposium on Naval Hydrodynamics*, Washington, D.C., USA, 1998.
- [16] Miyamoto, M., Sumikawa, J., Akiyoshi, T., and Nakamura, T., Effects of axial heat conduction in a vertical flat plate on free convection heat transfer, *Int. J. Heat and Mass Transfer*, Vol. 23, pp. 1545–1553, 1980.
- [17] Pozzi, A., and Lupo, M., The coupling of conduction with laminar natural convection along a flat plate, *Int. J. Heat and Mass Transfer*, Vol. 31, pp. 1807–1814, 1988.
- [18] Vynnycky, M., and Kimura, S., Transient conjugate free convection due to a heated vertical plate, *Int. J. Heat and Mass Transfer*, Vol. 39, pp. 1067–1080, 1996.
- [19] Nasif, G., Barron, R.M., and Balachandar, R., Simulation of piston cooling using oil jets, *Int. J. Heat and Mass Transfer*, 2014, Paper under review.
- [20] Cengel, Y.A., and Ghajar, A.J., *Heat and Mass Transfer: Fundamentals and Applications*, 4th Ed., McGraw-Hill, NY, USA, 2011.